

Ion injections at auroral latitude during the March 31, 2001 magnetic storm observed by Cluster

A. Korth,¹ M. Fränz,¹ Q.-G. Zong,² T. A. Fritz,² J.-A. Sauvaud,³ H. Rème,³ I. Dandouras,³ R. Friedel,⁴ C. G. Mouikis,⁵ L. M. Kistler,⁵ E. Möbius,⁵ M. F. Marcucci,⁶ M. Wilber,⁷ G. Parks,⁷ A. Keiling,³ R. Lundin,⁸ and P. W. Daly¹

Received 26 April 2004; revised 18 August 2004; accepted 23 September 2004; published 22 October 2004.

[1] We present here simultaneous H^+ and O^+ ion dispersion signatures observed by three Cluster spacecraft above the northern auroral zone. These observations occur during strong geomagnetic activity ($K_p = 9$) and are consistent with a time-of-flight (TOF) dispersion of the ions. Using the TOF dispersion of H^+ and O^+ and bouncing properties of H^+ , we show that the ions originate from a distant source located near $80 R_e$ down tail. Our results show that the magnetotail is topographically stable to support multiple bouncing of H^+ ions during a storm period. Furthermore these results could suggest that the plasmasheet H^+ and O^+ ions have been accelerated to the same velocity in the vicinity of a reconnection region. **INDEX TERMS:** 2700 Magnetospheric Physics; 2744 Magnetospheric Physics: Magnetotail; 2748 Magnetospheric Physics: Magnetotail boundary layers; 2764 Magnetospheric Physics: Plasma sheet; 2788 Magnetospheric Physics: Storms and substorms. **Citation:** Korth, A., et al. (2004), Ion injections at auroral latitude during the March 31, 2001 magnetic storm observed by Cluster, *Geophys. Res. Lett.*, *31*, L20806, doi:10.1029/2004GL020356.

1. Introduction

[2] The characteristics of impulsive dispersed proton bursts in the magnetotail (monotonic decrease of energy as a function of either time or increasing latitude) were first described by *Sarris and Axford* [1979] from in situ measurements taken inside the nightside plasma sheet. The energy dispersion signature has been explained by either a time-of-flight effect [*Sarris and Axford*, 1979; *Williams*, 1981; *Williams and Speiser*, 1984] of the energetic particles originating from a possible reconnection site, or by ions convecting into the magnetotail current sheet by $E \times B$ drift [*Zelenyi et al.*, 1990]. These ions get further accelerated and ejected following *Speiser* orbits [*Speiser*, 1967] from the

plasma sheet boundary layer (PSBL) and show an energy dispersion in the adjacent PSBL.

[3] Recently, similar ion energy dispersion phenomena were observed at low altitudes, above the auroral region during substorm periods by the Akebono and Interball satellites. TOF dispersion leads to either multiple bouncing proton clusters on closed field lines [*Hirahara et al.*, 1996] and/or to sporadic quasi-recurrent ejections of ions from an equatorial source [*Sauvaud et al.*, 1999]. The source distances were estimated between 8 and $40 R_e$. Here using the Cluster spacecraft we show that during strong magnetic activity, protons and oxygen can be ejected from the plasma sheet at distances as large as $80 R_e$. The recorded multiple bounces of protons indicate that the tail is topographically stable and the simultaneous observation of proton and oxygen ions suggest they received the same velocity impulse in the distant magnetotail, possibly near a reconnection region.

[4] To inspect the time dispersion effects we assume that the energy channels i and j show dispersion effects. The equation reads as follows

$$-T_i + T_0 + \frac{D}{v_i} = -T_j + T_0 + \frac{D}{v_j}$$

where T_i , T_j are the observed ion arrival times for the i , j energy channels having velocities v_i , v_j . The velocities are calculated for protons of different energies. T_0 is the onset time of the source, and D is the total distance from the source to the satellite.

[5] Assuming $v_i > v_j$ and $T_i < T_j$ to obtain the distance D , and the onset time T_0 of the source we have to solve the equation

$$T_j - T_i = D \left(\frac{1}{v_j} - \frac{1}{v_i} \right)$$

[6] Using for the first time multipoint measurements from the Cluster fleet, we have investigated the dispersed ion signature at different times in the auroral zone. In particular, we show structures of dispersed protons and oxygen during the large March 31, 2001 storm ($D_{st} = -387$ nT) and calculate the source distances of protons and oxygen during that storm.

2. Observations

[7] This study uses proton and oxygen ion measurements on three Cluster satellites SC1, SC3, and SC4 during the large magnetic storm on March 31, 2001 (data from SC2 not available). The Cluster satellites are in highly elliptical

¹Max-Planck-Institut für Sonnensystemforschung, Katlenburg-Lindau, Germany.

²Center for Space Physics, Boston University, Boston, Massachusetts, USA.

³Centre d'Etude Spatiale des Rayonnements, Toulouse, France.

⁴Los Alamos National Laboratory, Los Alamos, New Mexico, USA.

⁵Institute for the Study of Earth, Oceans, and Space, University of New Hampshire, Durham, New Hampshire, USA.

⁶Istituto di Fisica dello Spazio Interplanetario, Rome, Italy.

⁷Space Sciences Lab, University of California, Berkeley, California, USA.

⁸Swedish Institute of Space Physics, Kiruna, Sweden.

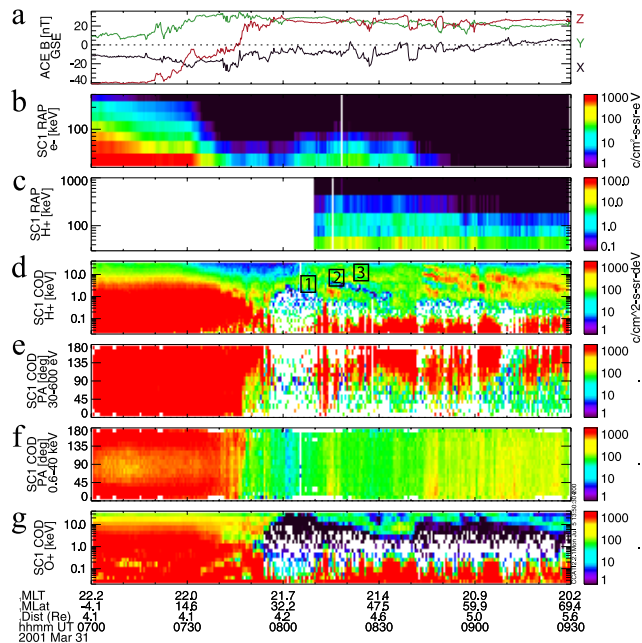


Figure 1. An overview plot of the storm main and recovery phase on March 31, 2001 from 07:00–09:30 UT. From top to bottom: ACE magnetic field without time shift, e^- and ion spectrograms from the Cluster RAPID instrument, and the proton spectrogram, two proton pitch angle distributions, and the oxygen spectrogram from the CIS instrument.

orbits, with apogee at 19.8 R_e and perigee of 4.0 R_e . On March 31, 2001 the Cluster satellites - flying like pearls on a string - recorded data near perigee in the northern auroral zone and northern lobe in the dusk-midnight sector approximately at 21 hours LT. The distance between SC1 and SC3 is about 600 km and between SC3 and SC4 about 1000 km.

[8] We use particle data from the CLUSTER Ion Spectrometry (CIS) plasma instrument, from the CLUSTER energetic particle spectrometer RAPID (Research with Adaptive Particle Imaging Detectors), and solar wind magnetic field data from the ACE satellite. Most of the data shown in this paper are from the Composition and Distribution Function (CODIF) analyzer, which is one of the sensors of the CIS instrument. CODIF measures the 3-dimensional distribution functions of the major ion species in the energy per charge range 20–40000 eV/e. CODIF can resolve the major ion species, H^+ , He^{++} , He^+ , and O^+ [Rème *et al.*, 2001]. The RAPID spectrometer performs species identification with a time-of-flight measurement in the energy range from 50 to 1500 keV [Wilken *et al.*, 2001].

[9] In Figure 1 we present an overview and some detailed Cluster observations during the large storm on March 31, 2001. The storm reached its minimum Dst value of -387 nT between 08:00 and 09:00 UT, commencing recovery subsequently. The Cluster satellites recorded data near perigee (~ 4.0 to $5.5 R_e$). Near perigee the spacecraft traverse first the outer radiation belt and the ring current, then the plasma sheet (northern auroral zone), the plasma sheet boundary layer (PSBL) and last the lobe in the dusk-midnight sector at approximately 21 hours MLT. The data show from top to bottom the magnetic field data from the ACE spacecraft ($\sim 210 R_e$ in front of the Earth) in GSE coordinates, the energetic electron and the proton spectro-

grams from the RAPID instrument on SC1, and the proton spectrogram, proton pitch angle distributions in two energy ranges and the oxygen spectrogram from the CIS-CODIF plasma instrument also from SC1. In Figure 1a the B_z component of the magnetic field (red line) changes sign at about 07:45 UT at L1. B_z will change sign at the magnetopause about 45–50 min later ($\sim 08:30$ – $08:35$ UT) which means that the convection stops in the tail. In Figures 1b, 1d, and 1g one can see that SC1 is in the outer radiation belt until about 07:40 UT. Between 07:40 UT and 08:00 UT ion beams from the plasma sheet are seen together with outflowing ions (Figures 1e and 1f). After 08:00 UT the ions show two different pitch angle distributions. The ions <600 eV are outflowing from the ionosphere whereas the ions >600 eV are streaming earthward and tailward and showing an energy-dispersed structure. The tailward streaming ions are simply the result of mirror point reflection earthward of the spacecraft. During large storms the outflow of oxygen can be very strong and most often larger than for protons. In this case the density ratio of O^+/H^+ amounts to 17 to 20 on the three spacecraft SC1, SC3, and SC4 in the time interval 08:10 to 09:00 UT. The dispersed energy structure of the protons measured by the CIS instrument up to energies of 38 keV find their energy continuation in the proton measurements of the RAPID instrument in Figure 1c. The RAPID ion measurements are switched automatically on only after 08:10 UT to protect the detectors from penetrating electrons in the radiation belt. In what follows we will concentrate on the time period 08:00 to 08:30 UT (21:30 MLT) in Figure 1 where we find three energy dispersed tracks which are marked by 1, 2, and 3. Track 1 shows a starting energy of about 5 keV and track 2 of about 10 keV after 7:50 UT. It seems that the Cluster satellites on the field line connected to the source miss the high energy ions. The ions from track 2 may have enough time to convect towards the central plasma sheet. The measured energy dispersions thus result from the added effects of time-of-flight dispersions and of convection.

[10] For Figure 2 the differential flux colour spectra from spacecraft SC1, SC3, and SC4 were taken for dispersion

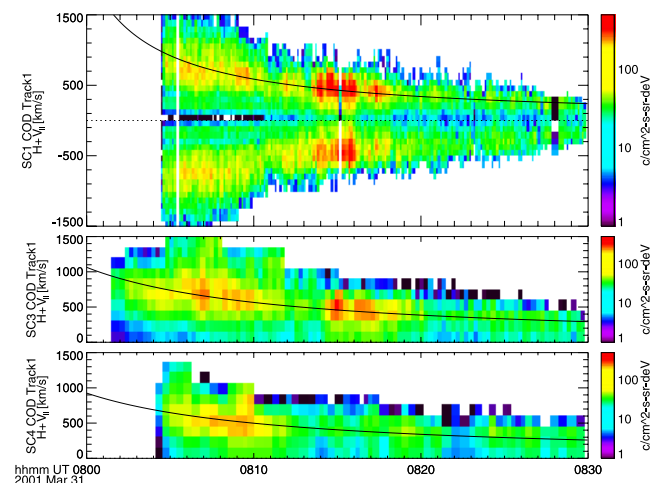


Figure 2. Proton parallel velocity spectrograms from SC1, SC3, and SC4 for dispersion track 1 (Figure 1) on March 31, 2001 from 08:00–08:30 UT. Overplotted are fitted hyperbolas $v = D/(t - t_0)$.

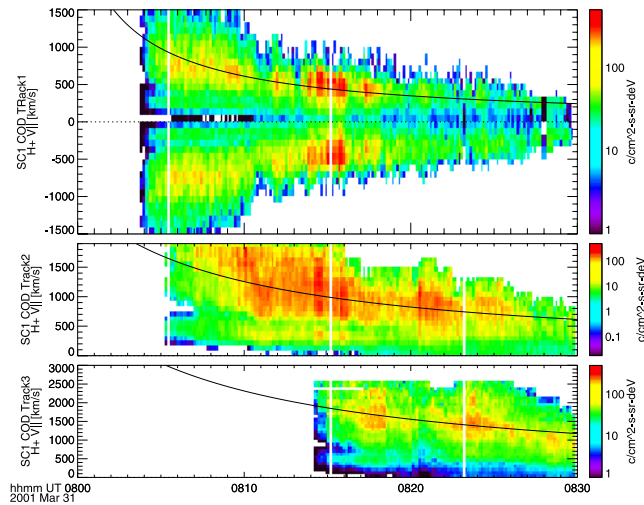


Figure 3. Proton parallel velocity spectrograms from SC1 for the dispersion track 1, 2, and 3 (Figure 1) on March 31, 2001 from 08:00–08:30 UT.

track 1 only. For track 1 the respective energy bins were marked by eye in the energy spectrogram. For all spatial sectors belonging to a selected energy bin the parallel velocity V_{\parallel} was calculated and the accumulated flux intensity for the V_{\parallel} bins was plotted in a V_{\parallel} parallel spectrum. V_{\parallel} positive is for protons coming along the field line - that is from the tail in our case. V_{\parallel} negative is for protons moving against the field direction. We assume that these are mirrored at the reflection point near the Earth and streaming tailward. The negative and positive velocity spectrograms are plotted only for SC1 which was switched on that day to the highest time and energy resolution. For SC3 and SC4 only the positive spectrograms are shown. For the $V_{\parallel} > 0$ branch the mean velocities are calculated for each time point and the reciprocals $1/v$ are fitted by linear regression with an error estimate calculated from the velocity spreads. The resulting hyperbolas $v = D/(t - t_0)$ give the source distance D and starting time t_0 for each particle track. The statistical error of the distance determination is $<10\%$ and smaller than the systematic error in the energy bin selection. The latter we determined by varying the bin selection. The starting times t_0 for track 1 agree with $t_0 = 7:52 \pm 4$ min. This variation also gives an upper limit for the size S of the source region. If we take an average ion speed for track 1 of $\bar{v} = 500$ km/s, we get $S < 8 \text{ min} \cdot \bar{v} \approx 40 R_e$. The source distance D for protons for the three Cluster SC is determined as $80 \pm 20 R_e$ tailwards.

[11] In Figure 3 parallel velocity spectrograms for protons from dispersion tracks 1, 2, and 3 are shown from spacecraft SC1. The calculations for the proton source distances give the following values: SC1 Track 1: $80 \pm 20 R_e$, SC1 Track 2: $220 \pm 40 R_e$, SC1 Track 3: $440 \pm 100 R_e$. The results can be interpreted such that the protons from track 1 are directly injected from the tail to the northern hemisphere, whereas the protons from track 2 are injected first to the southern hemisphere and then reflected at the southern mirror point and back via the tail to the northern hemisphere. This means that we get three times the source distance ($3 \times 80 R_e = 240 R_e$) of the directly injected protons. Protons from track 3 have conducted five bounces. The starting times t_0 for track

1, 2, and 3 agree with $t_0 = 7:52 \pm 4$ min, which means that Cluster is detecting only one event.

[12] Figure 4 repeats the V_{\parallel} spectrogram for protons from Figures 2 and 3 for reference. Figure 4b shows the oxygen spectrogram from the CIS-CODIF sensor from spacecraft SC1. Oxygen shows a similar dispersion as protons. However, there is only one dispersion track. The other two may be at higher energies and are not detected in the CIS instrument or are pitch angle scattered at the traversal of the neutral sheet, as expected from non-adiabatic motion. The RAPID instrument at higher energies has not enough energy resolution to resolve further tracks. In Figures 4c, 4d, and 4e the velocity spectrograms are plotted for oxygen streaming earthward (positive values) for the three spacecraft SC1, SC3, and SC4. Calculations of the source distance ($D = 82 \pm 12 R_e$) and starting times ($t_0 = 7:54 \pm 3$ min) for oxygen agree well within their errors with the proton source distance. It is assumed that the oxygen and proton source distances are identical and the source extension in the plasma sheet is quite large.

3. Discussion and Conclusions

[13] In agreement with the measurements by *Hirahara et al.* [1996] our observations show bouncing proton clusters. However, the source distance calculated from three Cluster spacecraft is much larger ($80 R_e$) than that obtained from Akebono data ($20\text{--}25 R_e$). This unexpected results shows that the tail topology is such that the protons can execute several bounces in the magnetotail keeping their first adiabatic invariant constant. This could be due to the overall disruption of the tail current during storm periods. Furthermore, H^+ and O^+ ions are both injected from the distant source. This suggests that the H^+ and O^+ ions are co-existing during this storm in the distant tail. The reason for the difference between Hirahara and our observations may thus be related to the different geomagnetic activity (large storm and substorm).

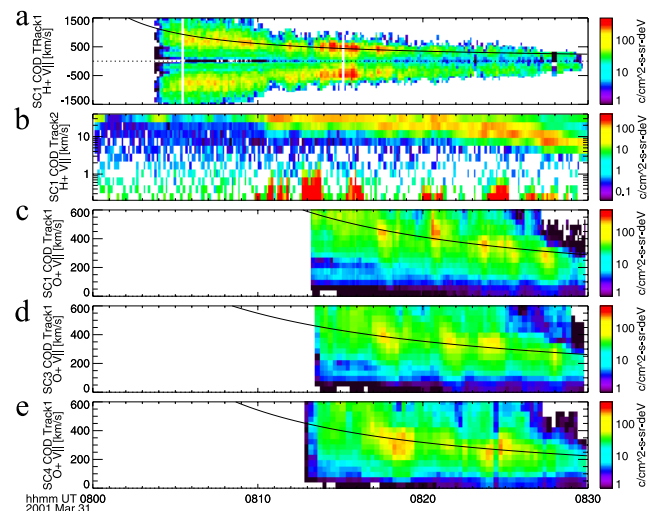


Figure 4. From top to bottom: Proton parallel velocity spectrogram from SC1 for dispersion track 1, CODIF oxygen spectrogram from SC1, and oxygen parallel velocity spectrograms from SC1, SC3, and SC4 on March 31, 2001 from 08:00–08:30 UT.

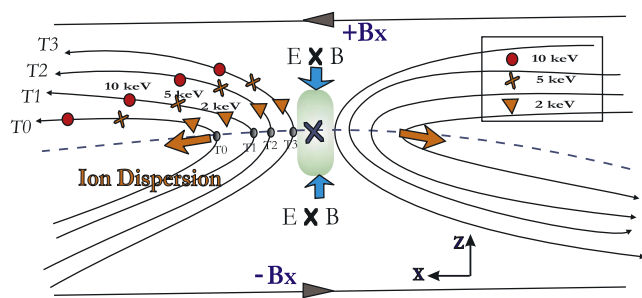


Figure 5. Schematic of reconnection process in the magnetospheric tail. The motion of magnetic field lines and the positions of the energetic ions released from the neutral line at the x -point and their progressive points. T_0 and the subsequent times T_1 , T_2 , T_3 refer to the ion release time for different field lines; 2, 5 and 10 keV are the assumed energy of the released ions by the acceleration process.

[14] A schematic illustration how the dispersed ions are generated in the distant tail by a progressive reconnection process is given in Figure 5. The energetic particles released from the reconnection region will result in energy-dispersed particles moving along the field lines, as observed with Cluster near perigee. A similar explanation has been given by Zong *et al.* [2001] for the dayside ion dispersion morphology during a reconnection process.

[15] The reconnected field lines carrying energetic ions move away from the diffusion region. Energetic ions on a given field line are accelerated more or less simultaneously, so that more energetic particles will be at any time further away from the reconnection region. During the reconnection process, the plasma bulk velocity is accelerated to the Alfvén velocity. The magnetic tension in the magnetotail applied by reconnection can add a velocity of the order of the Alfvén velocity, associated with the change in B . For a 10 nT field rotated by 180° , ΔB is 20 nT. Assuming a typical proton plasma density of 1 cm^{-3} in the tail plasma sheet, the Alfvén velocity is $\approx 490 \text{ km/s}$. A plasma sheet boundary region (last closed field lines) is formed by this reconnection process, and the accelerated ions are injected to the newly closed field lines. When the reconnection is fully developed and expanded, a layer of dispersed ions (protons and oxygen ions) can be observed in the near-Earth high latitude region.

[16] It is worthy to note, that different ion species originate from the same location as calculated from the observations (Figure 4). This is consistent with the view that all ion species have been accelerated to the same Alfvén velocity by the reconnection process.

[17] Finally, the main observations can be summarized as follows:

[18] 1. Multiple energy-dispersed ion structures are observed at auroral latitudes.

[19] 2. These structures happened during a large storm and substorm intensification (see Baker *et al.* [2002] for a detailed description of this period).

[20] 3. The energy dispersion can be explained as a time-of-flight effect of ions coming from the distant tail.

[21] 4. The multiple dispersed structures in the H^+ ions are due to multiple H^+ bounces.

[22] 5. The distance of the source region is $80 \pm 20 R_e$ and is similar for H^+ and O^+ .

[23] 6. The H^+ multiple bounces can only be supported by a topographically stable magnetotail at $\sim 80 \pm 20 R_e$.

[24] 7. The source extension in the plasma sheet is quite large but smaller than $40 R_e$.

[25] 8. The source can possibly be linked to a reconnection process affecting the tail.

[26] **Acknowledgments.** This RAPID-CLUSTER research was supported at Boston University by NASA grant NAG 5-10108. We thank the ACE magnetometer team at Bartol for providing ACE magnetometer data. We are grateful to the referees for suggesting important improvements to the paper.

References

- Baker, D. N., R. E. Ergun, J. L. Burch, J.-M. Jahn, P. W. Daly, R. Friedel, G. D. Reeves, T. A. Fritz, and D. G. Mitchell (2002), A telescopic and microscopic view of a magnetospheric substorm on 31 March 2001, *Geophys. Res. Lett.*, *29*(18), 1862, doi:10.1029/2001GL014491.
- Hirahara, M., T. Mukai, T. Nagai, N. Kaya, H. Hayakawa, and H. Fukunishi (1996), Two types of ion energy dispersions observed in the nightside auroral regions during geomagnetically disturbed periods, *J. Geophys. Res.*, *101*, 7749–7767.
- Rème, H., et al. (2001), First multispacecraft ion measurements in and near the earth's magnetosphere with the identical Cluster ion spectrometry (CIS) experiment, *Ann. Geophys.*, *19*, 1303–1354.
- Sarris, E. T., and W. I. Axford (1979), Energetic protons near the plasma sheet boundary, *Nature*, *460*, 277–279.
- Sauvaud, J.-A., D. Popescu, D. C. Delcourt, G. K. Parks, M. Brittacher, V. Sergeev, R. A. Kovrazhkin, T. Mukai, and S. Kokubun (1999), Sporadic plasma sheet ion injections into the high-altitude auroral bulge: Satellite observations, *J. Geophys. Res.*, *104*, 28,565–28,586.
- Speiser, T. W. (1967), Particle trajectories in model current sheets: 2. Applications to auroras using a geomagnetic tail model, *J. Geophys. Res.*, *72*, 3919–3932.
- Wilken, B., et al. (2001), First results from the RAPID imaging energetic particle spectrometer on board Cluster, *Ann. Geophys.*, *10*, 1355–1366.
- Williams, D. J. (1981), Ring current composition and sources: An update, *Planet. Space Sci.*, *29*, 1195–1203.
- Williams, D. J., and T. W. Speiser (1984), Source for energetic ions at the plasma sheet boundary: Time varying or steady state?, *J. Geophys. Res.*, *89*, 8877–8884.
- Zelenyi, L. M., A. Galeev, and C. F. Kennel (1990), Ion precipitation from the inner plasma sheet due to stochastic diffusion, *J. Geophys. Res.*, *95*, 3871–3882.
- Zong, Q. G., B. Wilken, S.-Y. Fu, T. A. Fritz, Z.-Y. Pu, N. Hasebe, and D. J. Williams (2001), Ring current oxygen ions in the magnetosheath caused by magnetic storm, *J. Geophys. Res.*, *106*, 25,541–25,556.

P. W. Daly, M. Fränz, and A. Korth, Max-Planck-Institut für Sonnensystemforschung, D-37191 Katlenburg-Lindau, Germany. (korth@lindpi.mpg.de)

I. Dandouras, A. Keiling, H. Rème, and J.-A. Sauvaud, Centre d'Etude Spatiale des Rayonnements, 9 Avenue du Colonel Roche, B.P. 4346, F-31028 Toulouse Cedex 4, France.

R. Friedel, Los Alamos National Laboratory, NIS-2, Mail Stop D-436, Los Alamos, NM 87545, USA.

T. A. Fritz and Q.-G. Zong, Center for Space Physics, Boston University, 725 Commonwealth Avenue, Boston, MA 02215, USA.

L. M. Kistler, E. Möbius, and C. G. Mouikis, Institute for the Study of Earth, Oceans, and Space, University of New Hampshire, 410 Morse Hall, Durham, NH 03824, USA.

R. Lundin, Swedish Institute of Space Physics, P.O. Box 812, SE-981 28 Kiruna, Sweden.

M. F. Marcucci, Istituto di Fisica dello Spazio Interplanetario, Area della Ricerca Tor Vergata, Via del Fosso del Cavaliere, 100, I-00133 Roma, Italy.

G. Parks and M. Wilber, Space Sciences Lab, University of California, Berkeley, CA 94720, USA.